ABCM Symposium Series in Mechatronics - Vol. 4 - pp.1-10

APPLICATION OF COMPUTER VISION AND KALMAN FILTERING TECHNIQUES TO IDENTIFY OIL FLAMES NEBULIZATION QUALITY

Fleury, A. T., agfleury@fei.edu.br
Centro Universitário da FEI
Escola Politécnica da Universidade de São Paulo

Trigo, F. C., flavio.trigo@poli.usp.br
Escola Politécnica da Universidade de São Paulo

Martins, F. P. R., flavius.martins@poli.usp.br
Escola Politécnica da Universidade de São Paulo

Abstract. *Vapor flow rate (VFR) is one of the main variables affecting the nebulization quality of oil flames in petroleum refinery furnaces. Too low values of VFR are directly correlated to a significant increase of the solid particulate material rate; as a consequence, the overall efficiency of the process decreases. As it has been observed, changes in VFR give rise to modifications of the flame visual patterns. Using characteristic vectors based on geometric properties of the gray level histogram of instantaneous flame images related to combustion processes with known a priori VFR values, feature vectors were calculated for all the images of a properly organized training set; then, a classification algorithm created a fuzzy measurement vector whose components represented membership degrees to the 'high nebulization quality' fuzzy set. Aiming at developing a real-time diagnostic system to describe the nebulization quality of the process when VFR is unknown, the fuzzy classification vector is assumed to be a state-vector in a random-walk model, and a Kalman filter attempts to predict this state after temporal input data issue. The successful validation of the output data, based on small training data sets, indicates that the proposed approach could be applied to synthesize a real-time algorithm dedicated to the evaluation of the nebulization quality of combustion processes developed in petroleum refinery furnaces that use oil flames as the heating source.*

Keywords*: Kalman filter; fuzzy logics; computer vision; combustion processes; petroleum refinery furnace*

1. INTRODUCTION

In order to project a control system that could improve the energetic efficiency of petroleum refinery furnaces and reduce the emission rate of pollutants — especially CO, NO_x and particulate material — it is necessary to set up a large network of heterogeneous sensors (thermocouples, flow meters, air-fuel ratio gauges, opacity meters, pressure sensors etc) dedicated to measure the main variables of the process and to give feedback to the controller. In the last two decades, however, video *CCD* cameras and frame grabbers have been incorporated to this measurement apparatus, since image sequences of flames captured by a near infra-red sensitive *CCD* and properly analyzed by suitable computer vision methods may provide a large quantity of useful information to the control. Correlations between the brightness, spectral and geometric properties of flame images and the corresponding variables of the combustion process have been reported by several authors, who developed different methods to build characteristic vectors and use them to estimate a subset of the state variables that characterize a combustion point of operation; consequently, it is expected that a computer vision based system may eventually replace the majority of the sensors used in traditional monitoring instrumentation of combustion processes.

Using average images of flames propagating inside glass furnaces operated at known *a priori* physical conditions, Santos-Victor *et al.* (1993) constructed a flame classification training set whose feature vectors were based on simple luminous and geometric properties of those images. The classification results generated by a Bayesian classifier and an *MLP* neural network with back propagation learning demonstrated that it was possible to identify the condition operation point of the furnace from simple estimations of the properties of their average images.

Tuntrakoon and Kuntanapreeda (1993), after establishing correlations between the colors of flames emanating from a premixed gas burner and the physical characteristics of the process, generated a pair of fuzzy rules based on triangular membership functions whose inputs measured the blue and orange content of *RGB* instantaneous images. Using those rules as a nonlinear controller, the authors have succeeded in implementing a real-time system to control the air and gas flow rates used in the combustion process.

Considering that the light intensity of the flame is proportional to combustion rate and, consequently, to heat release, Bertucco *et al.* (2000) developed an original computer vision based method to describe the hot spots dynamics, which may cause the rise of CO and NO_x emissions. Using a high speed camera to grab images at the frequency of 250 frames/s, these authors apply a sequence of thresholding and logical *AND* operators to a collection of sequential images, in order to identify the regions associated to high temperatures. A characteristic vector, based on geometric properties of these regions, is calculated, and the time series associated to each of its components, when represented in phase space, properly describes the vortex dynamics of the hot spots.

Baldini *et al.* (2000) investigated the correlation between parameters of image flames and the phenomenon of combustion instability that emerges when premixed combustors are used in industrial processes. After applying to each

instantaneous image a thorough segmentation process to separate the interest area (hottest zone of the flame) from the background, these authors constructed a characteristic vector based on some geometric properties of the isolated region. Considering the trend of those parameters as the measurements describing the temporal varying combustion process, their respective power spectra are generated and properly analyzed. As the relative importance of the characteristic vector parameters becomes explicit through the presence or absence of peaks in the spectra, a simple method to select the most significant parameters to control the process can be immediately elicited.

Yan *et al.* (2002) found out correlations between flame image measured parameters (area and centroid of the luminous region, ignition point position and spread angle) and physical data (particle size of the pulverized coals tested and mass flow rate of the primary air) and used them to build a characteristic vector of the combustion process. Working in the same project, Lu *et al.* (2004) added to the previous characteristic vector a flame flickering measure, based on the power spectral density of the temporal brightness of individual pixels. Later on, Lu *et al.* (2005) improved the characteristic vector with measures of the flame temperature distribution, using estimations based on 3D flame images reconstructed from 2D images captured by three 120^o separated cameras. Working on data and images proceeding from both laboratorial and industrial furnaces, these authors demonstrated that it is possible to monitor a real-time combustion process on the basis of a continuous analysis of flame images.

Sousa *et al.* (2003), in a previous project developed at IPT (Instituto de Pesquisas Tecnológicas do Estado de São Paulo - Brazil), proposed various computer vision algorithms to extract features of instantaneous and average flame images, in order to generate crisp decision rules that could be used to diagnose several kinds of abnormalities of the combustion process, encompassing flame extinction, lack of symmetry, instability, low nebulization quality and high or low excess air. Despite the good agreement between the decisions issued by the application of those rules to image test sets and the known *a priori* physical conditions concerning the capture of such images, three drawbacks of this diagnostic system must be pointed out: firstly, it required the calculation of average images and the application of heterogeneous computer vision methods to generate the parameters used by the majority of the diagnostic decision rules, what imposed a limitation to the system computational performance; secondly, only two states — either strict normality or abnormality of the process — could be diagnosed, although the decisions that can be made by a human expert on the combustion process are not so strict; finally, history of measurements were completely ignored, for the diagnostics were proposed on the basis of present measured values only.

Aiming at eliminating the above mentioned drawbacks, the referred combustion diagnostic system has been completely reformulated in this way: 1) computational performance has increased, since feature vectors based only on few properties of instantaneous images are used, and the algorithms applied to calculate such properties become simpler than those in Sousa *et al.* (2003); 2) fuzzy linguistic variables are used in the classification process, making the diagnostics more realistic; 3) decision-making becomes more robust, since predictions are obtained through a stochastic minimum variance least squares estimator.

Although the range of this diagnostic system encompasses five classes of abnormalities, as described above, only the modeling of nebulization quality diagnosis will be approached in this paper. It must be emphasized, however, that this parameter is of utmost importance in the combustion process, since low nebulization quality gives rise to an increase of the particulate material emission rate and to a decrease of the furnace thermal efficiency. As it will be described in the next topics, nebulization quality depends mainly on the vapor flow rate, defined as:

$$VFR = \frac{Q_v}{Q_o} \tag{1}$$

where Q_v refers to the nebulization vapor flow and Q_O to the fuel oil flow that compose the combustion mixture flow. It can be verified experimentally that low values of *VFR* are associated to combustion processes with low nebulization quality. Hence, as it will be explained below, this paper focuses on the development of an image-based diagnostic method to classify combustion processes according to its nebulization quality and to establish, by inference, an indirect correlation with the corresponding *VFR* value.

2. EXPERIMENTAL APARATUS

Experiments have been carried out at the IPT's Combustion Laboratory, where a comprehensive infrastructure to measure and actuate on the variables of combustion processes is fully available.

As illustrated in Fig. 1-a, the furnace used in the experiments is a vertical one, with the burner settled at the bottom and the gases exhaustion at the top. Having a total height of 4.0m, it is subdivided in 12 independent water cooled blocks and can process no. 1 fuel oil[1] at a maximum flow rate of 80 kg/h. The burner has two (primary and secondary) air entrances for natural air suction with manual flow regulation valves (Fig. 1-b).

[1] Fuel oil is classified into classes 1 to 6, according to its boiling point, composition and application. Number 1 fuel oils are distillated oils, i.e., they have low viscosity and are free of sediments and inorganic ash.

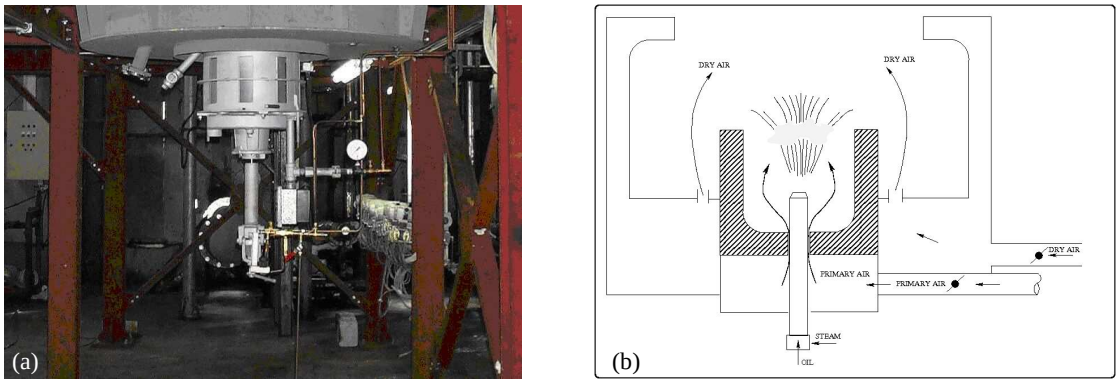

Figure 1. (a) Vertical furnace used in the experiments; (b) Burner schematics.

Flame images are generated by a standard monochromatic *RS-170 CCD* camera (Marshall Model 1070) using an objective lens (6mm, f1.2) supplied with a narrow band-pass (±10nm) interferometric filter at the 900 nm reference wave length, near to the sensitivity luminance peak (750 nm) of the *CCD* sensor and in the range of radiation of the soot, that corresponds to the major part of the radiation emitted by a typical fuel oil flame. All these optical components lie inside an air-water cooled housing with a double glass window, which is inserted into the furnace through a proper orifice (Fig. 2). The *CCD* camera output composed video signals are sampled at 25Hz by a frame grabber (Sensoray Model 611) as a series of interlaced 640x480 pixels images that are finally transferred to a Pentium-4 computer memory, using specific frame grabber driver functions.

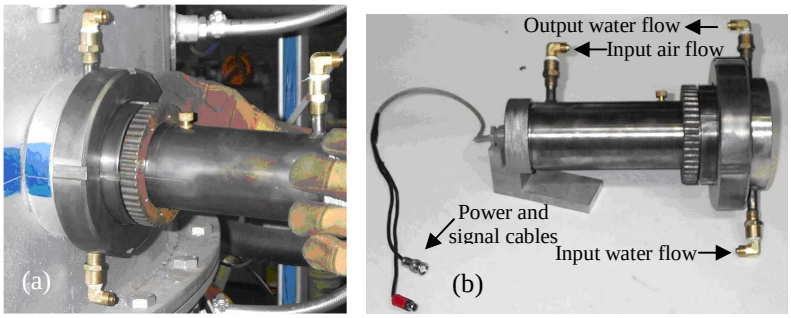

Figure 2. (a) Installation of the air-water cooled housing; (b) Housing details.

Flame images are processed by the image-based diagnostic system application, whose main tasks will be described in the next topics.

3. IMAGE FLAME ANALYSIS

Although combustion process characterization could be made on the basis of a large number of image feature properties, encompassing geometry, luminance and spectral aspects of the flame image, it was established that, to attend real-time performance requirements, only the simplest and fastest algorithms should be applied. Noticing that the shape of image gray-level histograms changed for flames with different nebulization qualities (Figs. 3-4), ten geometric properties of these histograms have been selected to compose the characteristic vector $\{v_i\}$ of a particular image flame I_i: v_{i1} = *x*-coordinate of the centroid; v_{i2} = *y*-coordinate of the centroid; v_{i3} = *x*-projection of the radius of gyration; v_{i4} = *y*-projection of the radius of gyration; v_{i5} = coordinate *x* corresponding to 33% of the accumulated area of the histogram; v_{i6} = coordinate *x* corresponding to 66% of the accumulated area of the histogram; v_{i7} = coordinate *x* of the highest peak of the histogram; v_{i8} = coordinate *y* of the highest peak of the histogram; v_{i9} = coordinate *x* of the second highest peak of the histogram; v_{i10} = coordinate *y* of the second highest peak of the histogram.

The characteristic vectors $\{v_i\}$ referred before have been calculated to every instantaneous image I_i of a training set with 214 deinterlaced flame images corresponding to nine different *VFR* values (0.17, 0.21, 0.23, 0.26, 0.29, 0.36, 0.43, 0.50, 0.57) associated to increasing nebulization qualities; at the same time, their respective fuzzy classifications to the fuzzy set *'Flames with high nebulization quality'* have been made by an expert in combustion processes (Fig. 5).

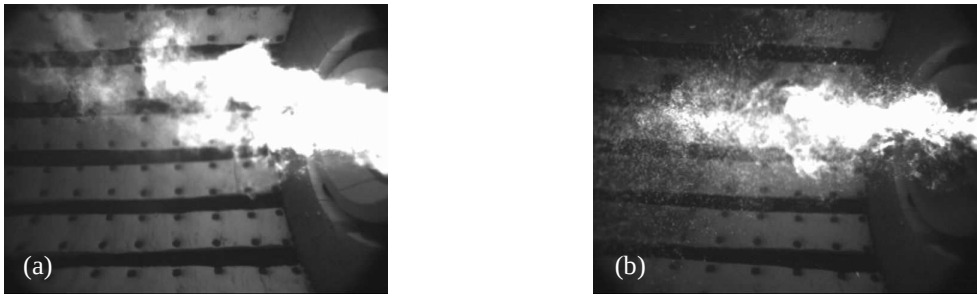

Figure 3. (a) Flame with high nebulization quality; (b) Flame with low nebulization quality.

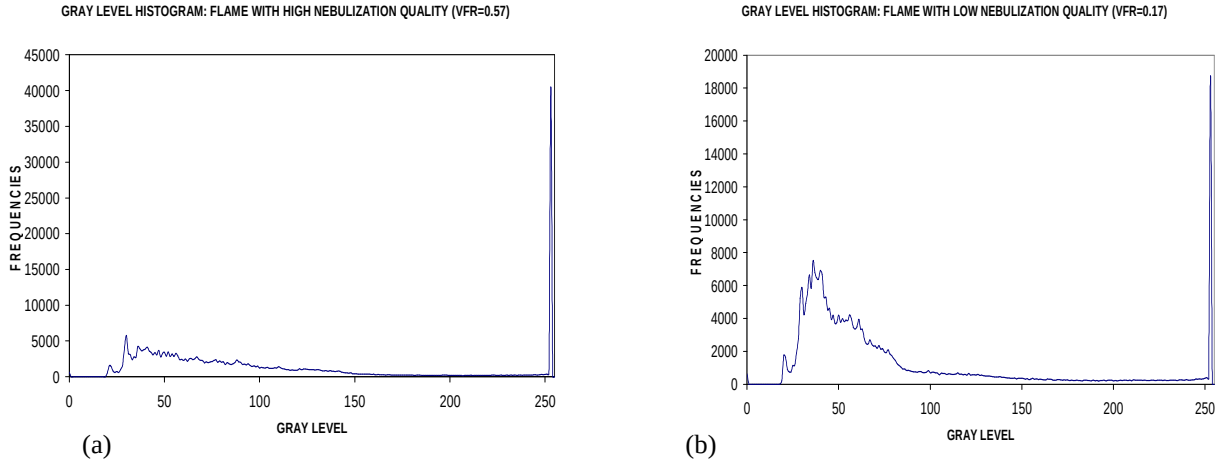

Figure 4. Gray level histograms of image flames: (a) High nebulization quality; (b) low nebulization quality.

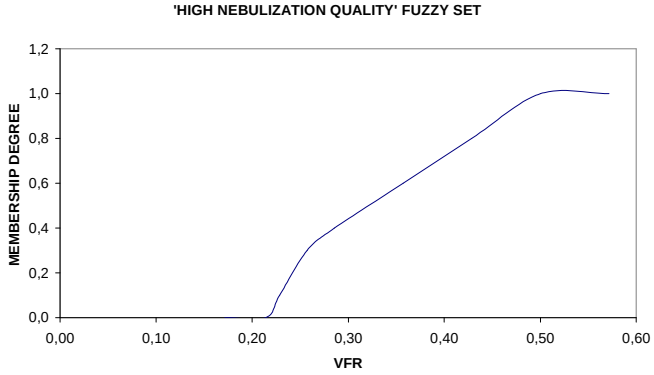

Figure 5. Fuzzy set associated to the 'High nebulization quality' concept.

After calculating the average histograms and the respective average characteristic vectors $\{\overline{v}_i\}(i=1,\cdots,9)$ for each of these nine image subsets, it has been established a straightforward method to determine the membership degree vector $\{x_i\}$ of a training set image I_i to the fuzzy set U = '*Flames with high nebulization quality*':

Let $v_{i,j}$ be an element of the matrix of 214 characteristic vectors $\{v_j\}$, where $j \in \{1,\ldots,9\}$. Then

for every vector $v_i, i=1,\ldots,214$,

for every component $v_{i,j}$, $j=1,\ldots,10$

calculate $d_j = \min\{|v_{i,j} - \overline{v}_{k,j}|\}, k=1\ldots 9$

determine $k_{\min} \mid d_j = \min\{|v_{i,j} - \overline{v}_{k,j}|\}, k=1\ldots 9$

determine $x_{i,j} = \mu(U, k_{\min})$

Applying the above fuzzy measurement algorithm, vector $\{x\}$ has been calculated for all the 214 images of the training set. Table 1 shows a collection of such measurements for five images of low nebulization quality, grabbed at *VFR* = 0.21.

Table 1: Membership degree vector $\{x\}$ to fuzzy set *U* = '*Flames with high nebulization quality*', calculated for images of low nebulization quality (*VFR*=0.21).

Images \ {x}	x_1	x_2	x_3	x_4	x_5	x_6	x_7	x_8	x_9	x_{10}
1	0,00	0,00	0,00	0,40	0,00	0,00	1,00	0,00	0,10	0,00
2	0,00	0,00	0,00	0,00	0,00	0,00	1,00	0,00	0,00	0,00
3	0,30	0,30	0,40	1,00	0,30	0,30	1,00	0,40	0,30	0,00
4	0,00	0,00	0,00	0,00	0,00	0,30	1,00	0,00	0,00	0,00
5	0,00	0,00	0,00	0,40	0,00	0,00	1,00	0,00	0,00	0,00

4. ESTIMATION PROBLEM

The literature presents some attempts to model the dynamics of flame propagation in a woodland fire through discretization of reaction-diffusion partial differential equations in one or two dimensions by finite differences and to estimate the state, the temperature distribution and the remaining amount of fuel, using the Ensemble Kalman Filter (Mandel *et al.*, 2008; Balbi, Santoni and Dupuy, 1999). Mandel *et al.*, for instance, generate synthetic ensembles for the Kalman Filter from the numerical solution of the reaction-diffusion equation. Combustion parameters of the model result from monitoring real woodland fire; as a result, the uncertainties are restricted to the PDE discretization. On the other hand, Hong, Yang and Ray (2000) simulate a state-space model of the truncated solution of the wave equation incorporating effects of acoustic waves and combustion dynamics in a generic gas-turbine engine combustion chamber. The researchers aim at designing a controller to cope with combustion instability, and their system model include uncertainties due to combustion parameters, model reduction (truncation) and boundary conditions. Both Mandel and Hong admit the difficulty in describing combustion behavior based on theoretical models. This brief discussion is meant to introduce and justify the approach this paper adopts.

The problem of determining the quality of flames is formulated as a state-estimation problem in which the state to be estimated is a vector containing ten image parameters obtained as described on the previous section. A linear Kalman filter is implemented to observe the state. Since a detailed discussion on stochastic estimation or on Kalman filtering theory is out of scope, only the main hypotheses and assumptions for applying the filter equations are stated. First of all, both the system and observation models must be in state-space form. The system model is given by a state equation that describes the evolution of the state, the ten-parameter vector in this case.

The difficulty that arises is: since those image parameters are geometric statistical properties of the gray level histogram, a physical relationship between them and the grabbed images is not straightforward. A model that can be used when there is little knowledge on the process is the random walk model, whose state-equation shows that system dynamics is governed by a noise vector, as given by the discrete-time equation, Eq. (2).

$$\{x(t_k)\} = [\Phi(t_k, t_{k-1})]\{x(t_k)\} + \{\omega(t_k)\} \tag{2}$$

where $\{x(t_k)\} \in \mathrm{R}^n$ is the state at the k^{th} time step kΔt, $[\Phi(t_k, t_{k-1})]$ is the transition matrix, in this case the identity matrix of order *n*, and $\{\omega(t_k)\} \sim \mathrm{N}(0, [Q(x(t_k))]) \in \mathrm{R}^n$ is a white zero-mean Gaussian noise vector with symmetrical positive semi-definite covariance matrix $[Q(x(t_k))] \in \mathrm{R}^{nxn}$, a necessary condition for Kalman filter implementation.

In order to build the observation model, it is taken for granted that each state-vector computed by the fuzzy classification algorithm carries an inherent uncertainty, which can be modeled as a measurement noise that corrupts the state-vector. Mathematically, then, measurements are given by Eq. (3),

$$\{y(t_k)\} = \{x(t_k)\} + \{\nu(t_k)\}, \tag{3}$$

where $\{y(t_k)\} \in \mathrm{R}^n$ represents the measurement at t_k, and $\{\nu(t_k)\} \sim \mathrm{N}(0,[R(y(t_k))]) \in \mathrm{R}^n$ is a white zero-mean Gaussian noise vector with symmetrical positive definite covariance matrix $[R(y(t_k))] \in \mathrm{R}^{nxn}$. The white sequences $\{\omega(t_k)\}$ and $\{\nu(t_k)\}$ are assumed mutually independent; therefore, as a consequence of being Gaussian, they are also uncorrelated among themselves. However, noise covariance matrices shall not be assumed diagonal, once it is possible to compute them from the available data, as it will be discussed in the next section.

Recursive estimation theory based on Kalman filtering is extensively discussed in the literature, see for instance Jazwinski (1970); thus, for the moment, it suffices to briefly describe the algorithm framework through its equations. For the model given by Equations (2) and (3), there is a forecast stage that seeks to produce the best estimates (in a stochastic least-squares sense) by propagating the previous estimated state based on the process model and its known (or admitted) statistics before new information is available. This way, Eq. (4)

$$\{\hat{x}(t_k)\}^f = \{\hat{x}(t_{k-1})\}^u \tag{4}$$

constitutes the state estimation forecast and Eq. (5)

$$[P]^f(x(t_k)) = [P]^u(x(t_{k-1})) + [Q(x(t_{k-1}))] \tag{5}$$

gives the estimation error covariance matrix forecast. When new data is available, an update stage provides proper correction to the forecasted estimates of the state and error covariance according to Equations (6) and (7),

$$\{\hat{x}(t_k)\}^u = \{\hat{x}(t_k)\}^f + [K_k]\left(\{y(t_k)\} - \{\hat{x}(t_k)\}^f\right) \tag{6}$$

$$[P(\hat{x}(t_k))]^u = ([I] - [K_k])[P(\hat{x}(t_k))]^f \tag{7}$$

The correction is provided by the Kalman gain matrix, computed by Eq. (8)

$$[K_k] = [P(\hat{x}(t_k))]^f ([P(\hat{x}(t_k))]^f + R(x(t_k)])^{-1} \tag{8}$$

thus completing the prediction-correction steps necessary for the next iteration.

5. NEBULIZATION QUALITY ESTIMATION

As it was stated on the previous section, the process covariance matrix $[Q(x(t_{k-1}))]$ to be included in Eq. (5) is calculated from available data in the following manner: According to the dynamical model from Eq. (2) and (3), state and measurement are the same for each training set (data set). It is admitted that the state, on each case, is corrupted by a white zero-mean Gaussian noise sequence that represents the uncertainty generated by the fuzzy measurement algorithm. In order to quantify this uncertainty, the complete history of state vector evolution, known for all sets, is assembled in a matrix $[X(x(t_k))] \in \mathrm{R}^{nxm}$, with n=10 (the dimension of the state vector) and m=214 (the complete history of state evolution); once it is done, the covariance of the state for the whole set of measurements, matrix $[\Gamma] \in \mathrm{R}^{nxn}$, can be computed according to Eq. (9)

$$[\Gamma] = E\{[X - E(X)].[X - E(X)]^T\} \tag{9}$$

The calculation of matrix $[\Gamma]$ involved data in the range from “high” to “low” nebulization quality characteristic experiments and, therefore, states the uncertainties of an actual process, whose nebulization quality is unknown *a priori*; on that ground, although the actual state covariance for a particular set is not available, matrix $[\Gamma]$ is assumed to be an estimator of matrix $[Q]$ for each individual process, thus completing the random walk model for the state evolution.

As to the observation model, measurements are synthetically generated for each set by adding to the state a white zero-mean Gaussian noise sequence with 10% of the maximum value assumed by the state variables throughout the process. The noise sequence is calculated using a routine from Press *et al.* (2002), operating within a self-made driver.

The estimation procedure was evaluated by running the Kalman filter algorithm with the model from Eq. (2) and (3), state covariance matrix $[Q]$ and measurement noise covariance matrix $[R]$ computed by Eq. (9) using vector $\{y\}$ instead of matrix $[X]$, and using three training sets, namely *VFR* = 0.17, 0.29 and 0.5, respectively reproducing "low", "medium" and "high" quality nebulization conditions. The initial state vector assumes a "high" nebulization quality, i.e., the state variables are given the value 1.0. Initial error covariance matrix, $[P_0]$, is assumed diagonal with variances 0.3 for all experiments.

Validation of the process is achieved by comparing the estimates for the three training sets with their expected fuzzy measured values.

6. RESULTS AND DISCUSSION

Estimates obtained with the proposed approach for the three situations appear in Figures 6, 7 and 8, in which the evolution of every state variable is separately represented with coloured lines. In order to classify nebulization quality, we averaged state variables for every time step and plotted it with a bold black line with triangle markers; this way, it is possible to visualize the trend of the state vector throughout the process.

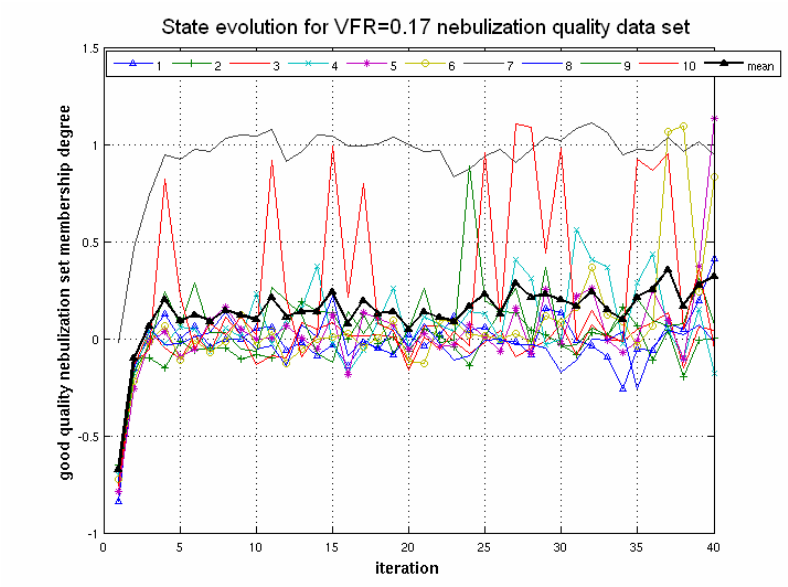

Figure 6: State evolution for *VFR*=0.17 nebulization quality data set.

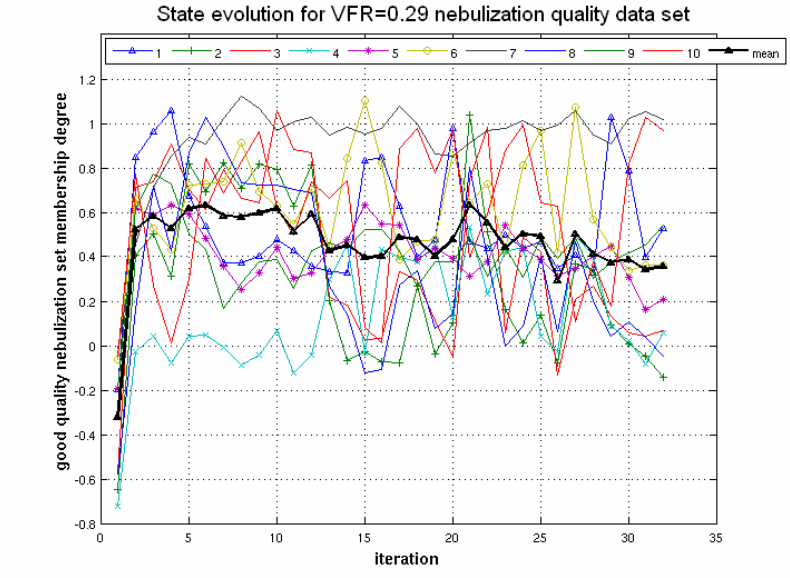

Figure 7: State evolution for *VFR*=0.29 nebulization quality data set.

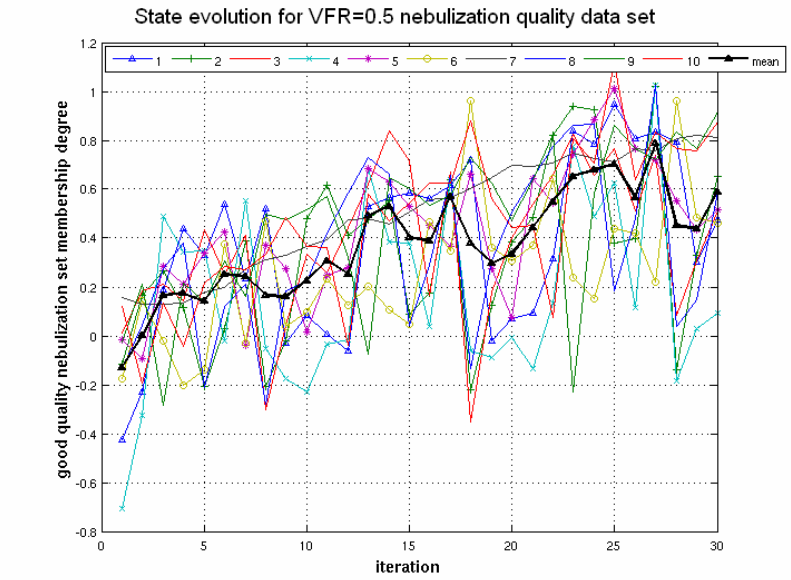

Figure 8: State evolution for *VFR*=0.5 nebulization quality data set.

The mean values for the state estimates obtained from data reproducing the *VFR*=0.17 (“low” nebulization quality), Figure 6, show that the process converges after 5 iterations to values ranging from 0.0 to 0.3, meaning that the estimated nebulization quality, in average, agreed with the expected result. However, the behavior of state variable no. 7, plotted in brown line, is not in accordance with the expectation for the following reason: It corresponds to the 253 pixel gray level, that is the most frequent for all images, since the relatively low dynamic range of the *CCD* camera used in the experiments gives rise to images with luminance saturated pixels at the higher gray levels. As similar behavior for this state variable is observed in Figures 7 and 8, one concludes that it is unable to distinguish nebulization quality features. On the other hand, it asserts the proper implementation of the Kalman filter for the three processes, since it represents a forcing term that actually converges for the recurrent value, 1.0 in average.

The “medium” and “high” nebulization qualities are estimated respectively after 15 and 25 iterations of the Kalman filter processing data from *VFR*=0.29 and *VFR*=0.5, as depicted by the bold black line in Figures 7 and 8. Figure 7 shows that the estimates of average state variables oscillate around 0.45, whereas in Figure 8 the bold black line has a positive decreasing gradient towards the “high” nebulization range. Despite those results, actual convergence of the estimation process must be asserted by the inspection of the observation residuals (Jazwinski, 1970), the difference between the effective measurement and its value as calculated by the filter using the last available state estimate. An estimation process is considered convergent once the normalized observation residuals is zero-mean Gaussian with standard deviation between $-3\sigma_\nu$ and $3\sigma_\nu$, given by Eq. (10)

$$r_\nu = \frac{1}{\ell\sigma_\nu}\sum_{j=1}^{\ell}(\{y(t_k)\}-\{\hat{x}^f(t_k)\}) \,, \tag{10}$$

where ℓ represents measurement vector dimension (Fleury, 1985). In Figure 9, it is shown that those requirements are fulfilled for experiments with *VFR* set to 0.17 and 0.29; therefore, one concludes that they converge. In relation to *VFR*=0.50 experiment, the mean criterion is not accomplished. A possible explanation is the reduced number of measurements available for procedure validation. Nevertheless, one observes that the triangle-marked curve has a clear tendency towards the null value.

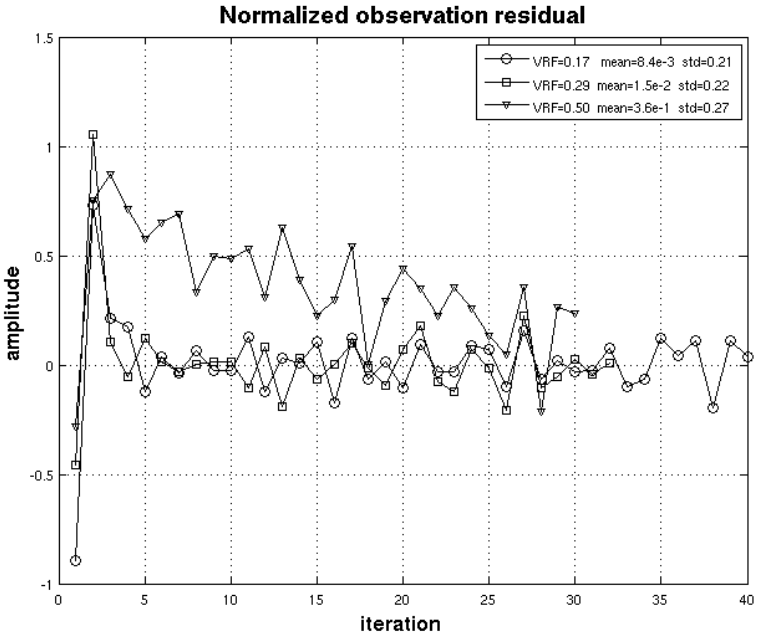

Figure 9. Normalized observation residuals

7. CONCLUSION

This work has investigated a method that potentially allows the classification of nebulization quality of oil flames in industrial processes. The method is based on the prediction of the dynamic behavior of a characteristic vector of parameters extracted from the gray level histogram of instantaneous flame images by the application of a fuzzy measurement algorithm to those images. A state-space approach through the Kalman filter provided estimates of image parameter vectors from data including experimental results of all the training image sets, reproducing several nebulization quality conditions.

Validation of the method was accomplished by comparing those estimates with experimental data for which the nebulization quality, according to a definite *VFR*, was previously known. Results show that the filter estimates can be considered statistically convergent towards their expected values after few iterations. Since the computational time necessary to generate the histograms and the estimates for the parameter vector is on the order of nanoseconds, the only limitation for using the method as a real-time monitor of the combustion process nebulization quality is the image sampling rate. For instance, the experimental apparatus described in this paper is able to grab images at a frequency of 25 Hz and, as it took the estimation algorithm at most 20 iterations to track the state, nebulization quality is determined in less than one second.

We stress that, despite the poor state model used, the results obtained are promising; this suggests that such a method could be applied to real-time monitoring the nebulization quality of an oil refinery furnace, with the following advantages over conventional methods: (*i*) the instrumentation setup is based on a single *CCD* camera; (*ii*) measurements are simple properties of the gray level histogram of flame instantaneous images; (*iii*) diagnostics consider the time history of the process.

8. ACKNOWLEDGEMENTS

This work was supported by CNPq as part of the project 471115/2004-5, “Sistema de Monitoramento em Tempo Real de Chamas em Forno de Refino". First author also gratefully acknowledges CNPq for financial support.

9. REFERENCES

Balbi, J.H., Santoni, P.A., and Dupuy, J.L., 1999. ``Dynamic modeling of fire spread across a fuel bed", International J. of Wildland Fire, vol. 9, Nr. 4, pp. 275-284.

Baldini, G., Campadelli, P., Lanzarotti, R., 2000. “Combustion Analysis by Image Processing of Premixed Flames”. Proceedings of the International Conference on Image Processing 2000, Vol.2, Vancouver, Canada, pp. 708-711.

Bertucco, L., Fichera, A., Nunnari, G., Pagano, A., 2000. “A Cellular Neural Networks Approach to Flame Image Analysis for Combustion Monitoring”. Proceedings of the 2000 6th IEEE International Workshop on Cellular Neural Networks and their Applications, Catania, Italy, pp. 455-459.

Fleury, A. T., 1985. “Estimadores de Estado de Sistemas Dinâmicos Baseados no Conceito de Dualidade”. Tese (Doutorado), Universidade de São Paulo,

Hong, B., Uang, V., and Ray, A., 2000. “Robust Feedback Control of Combustion Instability with Modeling Uncertainty”, Combustion and Flame, vol. 120, pp. 91-106.

Jazwinksi, A.H., 1970, ``Stochastic Processes and Filtering Theory", Academic Press, New York, USA, 376 p.

Lu, G., Yan, Y., Colechin, M., 2004. “A Digital Imaging Based Multi Functional Flame Monitoring System”. IEEE Transactions on Instrumentation and Measurement, Vol.53, No.4, pp. 1152-1158.

Mandel, J., Bennethum, L.S., Beezley, J.D., Coen, J.L., Douglas, C.C., Kim, M., and Vodacek, A., 2008. “A Wildland Fire Model with Data Assimilation”, Mathematics and Computers in Simulation, vol. 79, pp. 584-606.

Press, W., Vetterling, W.T., Teukolsky, S.A., and Flannery, B.P., 1992, 2nd. Ed. “Numerical Recipes in C: The Art of Scientific Computing”, Cambridge University Press, Cambridge, U.K., 994 p.

Santos-Victor, J. A., Costeira, J.P., Tomé, J.A.B., Sencieiro, J.J.S., 1993. “A Computer Vision System for the Characterization and Classification of Flames in Glass Furnaces”. IEEE Transactions on Industry Applicationa, Vol.29, No. 3, pp. 470-478.

Sousa, F.D.A., Martins, F.P.R., Bruna, W.C., 2003, “Desenvolvimento de Sistemas Avançados de Monitoração em Fornos de Refino”. Relatório Técnico IPT No. 67.109, 131 pg.

Tuntrakoon, A., Kuntanapreda, S., 2003. “Image Based Flame Control of a Premixed Gas Burner Using Fuzzy Logics”. Lecture Notes in Computer Science: Foundations of Intelligent Systems, Maebashi City, Japan, pp. 673-677.

Yan, Y., Lu, G., Colechin, M., 2002. “Monitoring and Characterization of Pulverized Coal Flames Using Digital Imaging Techniques”. Fuel, 81, pp. 647-656.

Yu, H., MacGregor, J. F., 2004. “Monitoring Flames in an Industrial Boiler Using Multivariate Image Analysis”. AIChE Journal, Vol.50, No.7, pp.1474-1483.

5. RESPONSIBILITY NOTICE

The authors are the only responsible for the printed material included in this paper.